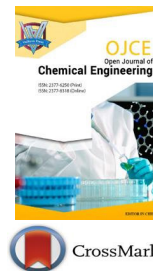




ISSN: 2377-6250 (Print)
ISSN: 2377-8318 (Online)
CODEN : OJCEB4



ARTICLE

ONE-POT SYNTHESIS OF EU-DOPED Ni-Fe LDH AND ENHANCED ELECTROCATALYTIC OXYGEN EVOLUTION PERFORMANCE

Xiangmeng Chen¹, Lu Lin¹, Linlin Li¹, Shengqiang Guo¹, Guanyan Li¹, Limin Wang¹, Hanyin Li¹, Fei Wang¹, Limin Guo¹, Yifeng He¹, Guanyan Li¹, YuTong Wang², Yiling Yang³, Xiaoxia Wu^{1*}

¹College of Science, College of Forestry, College of Food and Technology, Henan Agricultural University, Zhengzhou 450002, China

²College of Materials Science and Engineering, Nanjing Forestry University, Nanjing 210037, China

³First Affiliated Hospital of Zhengzhou University, Zhengzhou 450000, China

*Corresponding Author E-mail: Wuxiaoxia@163.com

This is an open access article distributed under the Creative Commons Attribution License, which permits unrestricted use, distribution, and reproduction in any medium, provided the original work is properly cited.

ARTICLE DETAILS

ABSTRACT

Article History:

Received 5 August 2022
Accepted 12 November 2022
Available online 30 December 2022

Hydrogen production via water electrolysis is critical for addressing energy and environmental challenges, but the oxygen evolution reaction (OER) requires efficient, stable, and low-cost electrocatalysts. Layered double hydroxides (LDHs) show promise for OER but suffer from insufficient active site utilization and conductivity. Herein, seven rare earth ions (La, Ce, Eu, etc.)-doped nickel-iron layered double hydroxide (Ni-Fe) LDH nanomaterials were fabricated via a one-pot co-precipitation method. Characterizations (X-ray diffraction (XRD), scanning electron microscopy (SEM), and electrochemical tests) demonstrated successful rare earth doping without damaging the LDH layered structure, with Eu-Ni-Fe LDH exhibiting optimal catalytic performance. Specifically, 15% Eu-doped Ni-Fe LDH achieved an overpotential of 196.8 mV at 10 mA·cm⁻² in 1.0 mol/L KOH, a Tafel slope of 134.63 mV·dec⁻¹, a double-layer capacitance (C_{dl}) of 12.94 mF·cm⁻², and excellent stability over 50 h. This study provides a novel strategy for modifying LDH-based OER catalysts and expands their renewable energy application potential.

KEYWORDS

One-pot method; rare earth doping; Ni-Fe layered double hydroxide; oxygen evolution reaction; electrocatalyst

1. INTRODUCTION

With the increasing severity of the global energy crisis and environmental pollution, hydrogen energy, as a clean and renewable energy source, has emerged as one of the core directions for the future energy system [1,2]. Water electrolysis for hydrogen production is widely recognized as the most promising technology due to its zero carbon emissions and high product purity. However, the anodic oxygen evolution reaction (OER) involves a complex multi-electron transfer process, which is characterized by high overpotential and sluggish reaction kinetics, thereby severely limiting the overall efficiency of water electrolysis [3,4]. Currently, commercial OER catalysts primarily rely on noble metals such as ruthenium (Ru) and iridium (Ir); the scarcity and high cost of these noble metals hinder their large-scale industrial application. Therefore, the development of high-performance and low-cost non-noble metal OER catalysts has become a key research focus in the field [5-7].

Layered double hydroxides (LDHs) are a class of two-dimensional layered materials with a hydrotalcite-like structure, consisting of positively charged metal hydroxide layers and interlayer counter anions. They possess distinct advantages, including adjustable elemental composition, large specific surface area, and abundant active sites, which make them promising candidates for OER catalysis [8,9]. Among various LDH materials, nickel-iron layered double hydroxide (Ni-Fe LDH) has become one of the most promising alternatives to

noble metal catalysts due to its excellent OER activity and low cost [10]. Nevertheless, its practical application is limited by inherent drawbacks such as low electrical conductivity, insufficient exposure of active sites, and poor cyclic stability [11].

Rare earth elements (La-Lu, Sc, Y) are characterized by unique 4f electron configurations, diverse valence states, and strong oxygen affinity. As dopants, rare earth elements can effectively regulate the electronic structure of catalysts, induce lattice defects, increase the number of active sites, and thereby enhance the catalytic activity and stability of catalysts [12]. Additionally, the one-pot synthesis method offers distinct advantages of simple operation, low cost, and environmental benignity, which enables uniform doping of rare earth ions in Ni-Fe LDH and avoids impurities and structural defects caused by multi-step synthesis processes [13].

Based on the aforementioned considerations, seven types of rare earth ion-doped Ni-Fe LDH catalysts were prepared via a one-pot method in this study. The effects of rare earth element types and Eu doping content on the material structure and OER catalytic performance were systematically explored, and the intrinsic mechanism by which rare earth doping modulates the electrochemical performance of Ni-Fe LDH was clarified. This work provides theoretical support and technical references for the design and preparation of high-performance LDH-based OER catalysts.

2. EXPERIMENTAL MATERIALS

2.1 Materials

Iron nitrate ($\text{Fe}(\text{NO}_3)_3 \cdot 6\text{H}_2\text{O}$) and nickel nitrate ($\text{Ni}(\text{NO}_3)_2 \cdot 6\text{H}_2\text{O}$) were purchased from Shanghai Macklin Biochemical Technology Co., Ltd. Rare earth nitrates, including lanthanum nitrate ($\text{La}(\text{NO}_3)_3 \cdot 6\text{H}_2\text{O}$), cerium nitrate ($\text{Ce}(\text{NO}_3)_3 \cdot 6\text{H}_2\text{O}$), and europium nitrate ($\text{Eu}(\text{NO}_3)_3 \cdot 6\text{H}_2\text{O}$), were obtained from Shanghai Titan Technology Co., Ltd. Urea ($\text{CO}(\text{NH}_2)_2$), ammonium fluoride (NH_4F), hydrochloric acid (HCl), and other reagents were of analytical grade, purchased from Sinopharm Chemical Reagent Co., Ltd. and other reputable suppliers.

2.2 Characterization

Crystal structure characterization: X-ray diffraction (XRD) was employed to analyze the phase composition of the samples, with a scanning range of 10° - 80° and a scanning rate of $5^\circ/\text{min}$. Morphology and element analysis: Scanning electron microscopy (SEM) was used to observe the morphology of the samples, and energy dispersive spectroscopy (EDS) was conducted to examine the elemental distribution and content in the samples. Electrochemical performance testing: Electrochemical measurements were performed using a three-electrode system, with 1.0 mol/L KOH solution as the electrolyte, a Pt sheet as the counter electrode, a saturated calomel electrode as the reference electrode, and nickel foam loaded with the catalyst as the working electrode. Linear sweep voltammetry (LSV), Tafel analysis, electrochemical impedance spectroscopy (EIS), cyclic voltammetry (CV), and stability tests were carried out in sequence. All measured potentials were calibrated to the reversible hydrogen electrode (RHE), and the overpotential (η) was calculated using formula (1).

$$\eta = E(\text{RHE}) - 1.23 \text{ V} \quad (1)$$

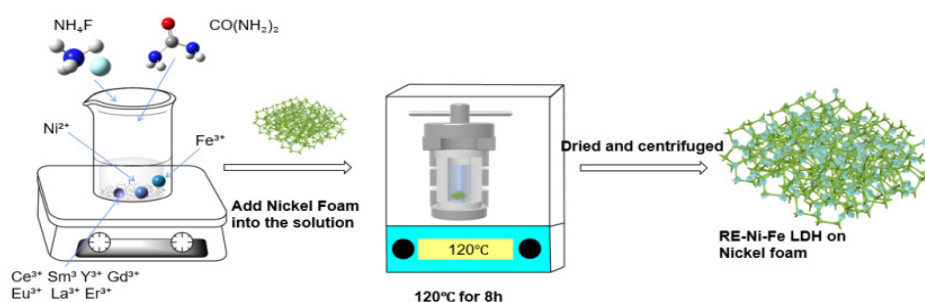


Figure 1: Rare earth-doped Ni-Fe LDH preparation flowchart.

2.3 Material preparation

2.3.1 Pretreatment of nickel foam

Nickel foam was cut into slices with dimensions of $3.0 \text{ cm} \times 1.0 \text{ cm}$. The slices were ultrasonically cleaned with 3 mol/L HCl, acetone, and absolute ethanol for 30 min each to remove surface oxide layers and impurities. Subsequently, the cleaned nickel foam slices were dried in a vacuum drying oven at 60°C for 4 h and stored in a dry environment for further use.

2.3.2 Preparation of rare earth-doped Ni-Fe LDH

Seven types of rare earth ions (La^{3+} , Ce^{3+} , Eu^{3+} , etc.)-doped Ni-Fe LDH were synthesized via the one-pot method, and the detailed procedure is shown in Figure 1. First, seven beakers were prepared, each containing 6 drops of 3 mol/L HCl and 20 mL of deionized water. Subsequently, 0.5 mmol $\text{Fe}(\text{NO}_3)_3 \cdot 6\text{H}_2\text{O}$, 1.5 mmol $\text{Ni}(\text{NO}_3)_2 \cdot 6\text{H}_2\text{O}$, and 0.4 mmol of the corresponding rare earth nitrate were added to each beaker, followed by uniform stirring until complete dissolution. Separately, another seven beakers were prepared by dissolving urea and ammonium fluoride in 10 mL of deionized water; the resulting solutions were slowly poured into the aforementioned mixed solutions, and the pH value of each mixture was adjusted to 3, followed by continuous stirring for 30 min. The mixed solutions were then transferred to 100 mL polytetrafluoroethylene autoclaves and reacted at 120°C for 8 h. After natural cooling to room temperature, the products were centrifuged and washed with deionized water three times, then dried in a vacuum drying oven at 60°C for 4 h to obtain rare earth-Ni-Fe LDH powder samples with a doping content of 20%. Using the same experimental procedure, Eu-Ni-Fe LDH samples with Eu doping contents of 2.5, 5, 7.5, 10, 15, and 20% were prepared to investigate the influence of Eu doping content on the catalytic performance of the materials.

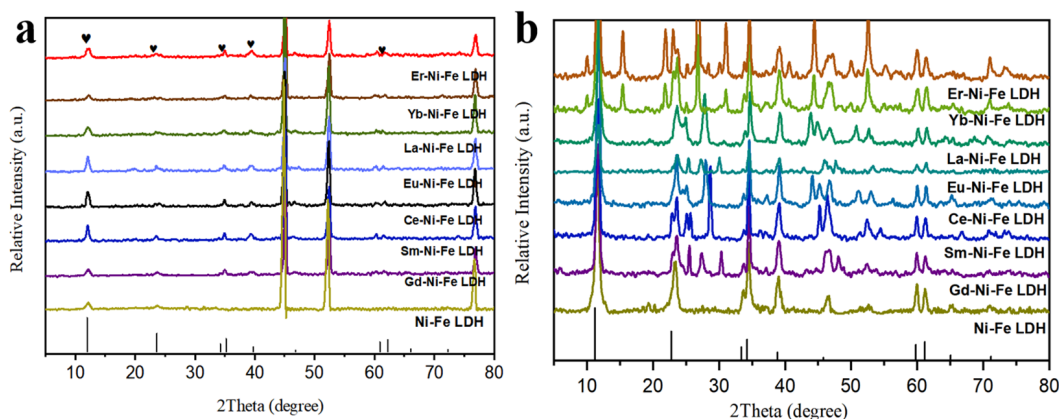


Figure 2: XRD diagram of Ni-Fe LDH with (a) foam nickel loading and (b) powdered original doped rare earth ions.

3. RESULTS AND DISCUSSION

3.1 Crystal structure analysis

All samples exhibit the characteristic diffraction peaks of Ni-Fe LDH (JCPDS Card No. 00-040-0215), as illustrated in the XRD patterns of pristine Ni-Fe LDH and seven rare earth-doped Ni-Fe LDH samples (Figure 2). The diffraction peak at 11.4° corresponds to the (003) crystal plane of LDH, while the diffraction peaks at 23.0° , 33.5° , and 34.4° are attributed to the (006), (012), and (015) crystal planes, respectively [14]. This result indicates that rare earth doping does not destroy the layered crystal structure of Ni-Fe LDH.

When comparing different rare earth-doped samples, slight shifts in the positions of some characteristic diffraction peaks are observed. For instance, the (003) crystal plane peaks of Ce-Ni-Fe LDH and Sm-Ni-Fe LDH differ slightly. This phenomenon is mainly attributed to the different ionic radii of rare earth elements (Ce^{3+} and Sm^{3+} have distinct ionic radii); after doping, these rare earth ions replace $\text{Ni}^{2+}/\text{Fe}^{3+}$ in the LDH layers, leading to minor changes in lattice parameters [15]. Additionally, the intensity of the characteristic diffraction peaks does

not decrease significantly after rare earth doping, suggesting that the crystallinity of the material remains excellent, which further confirms the successful doping of rare earth ions into the layered structure of Ni-Fe LDH.

3.2 Morphology and element distribution analysis

The SEM images, together with the EDS elemental distribution maps of the Eu-Ni-Fe LDH samples, are displayed in Figure 3. As shown, Eu-Ni-Fe LDH exhibits a typical two-dimensional nanosheet structure [20], with the nanosheets stacking to form a flower-like morphology, which is consistent with that of pristine Ni-Fe LDH. This result confirms that Eu doping does not damage the characteristic layered structure of LDH. The flower-like stacked structure can effectively increase the specific surface area of the material, provide more active sites for the OER process, and facilitate electrolyte penetration and product desorption. The EDS elemental distribution maps reveal that Ni, Fe, Eu, and O elements are uniformly distributed throughout the sample. The clear detection of Eu element further verifies the successful and uniform doping of Eu ions into the Ni-Fe LDH structure without agglomeration, which provides a reliable structural guarantee for its excellent catalytic performance.

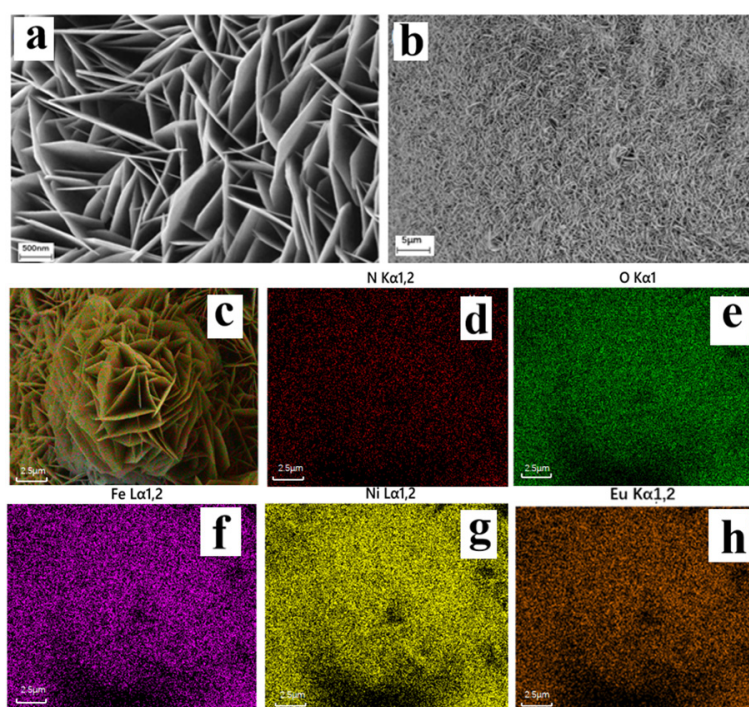


Figure 3: Element distribution map of Eu-Ni-Fe LDH.

3.3 Electrochemical catalytic performance analysis

3.3.1 Effect of different rare earth doping on oer performance

The LSV curves of pristine Ni-Fe LDH and seven rare earth-doped Ni-Fe LDH samples, along with their overpotential comparison at a current density of $10 \text{ mA}\cdot\text{cm}^{-2}$, are presented in Figure 4. It is apparent from these curves that all rare earth-doped samples possess lower initial subsequent decrease in catalytic activity.

3.3.2 Effect of Eu doping amount on OER performance

Comparative analysis of the LSV curves and Tafel slopes for Eu-Ni-Fe LDH samples with varying Eu doping contents is provided in Figure 4. A notable dependence of catalytic performance on Eu doping content is observed, where catalytic activity initially enhances and subsequently declines with increasing Eu doping level. The optimal catalytic performance is attained when the Eu doping content is 15%, with the sample exhibiting an overpotential of 196.8 mV at a current density of $10 \text{ mA}\cdot\text{cm}^{-2}$ and a Tafel slope of $134.63 \text{ mV}\cdot\text{dec}^{-1}$, markedly lower than

the Tafel slope of pristine Ni-Fe LDH ($156.97 \text{ mV}\cdot\text{dec}^{-1}$). A lower Tafel slope indicates faster OER reaction kinetics and higher charge transfer efficiency [18]. The low Tafel slope of 15% Eu-Ni-Fe LDH suggests that Eu doping can effectively accelerate charge transfer during the OER process and improve reaction kinetics. However, when the Eu doping content exceeds 15%, excess Eu ions occupy the active sites in the Ni-Fe LDH layers, leading to a reduction in the number of active sites and a subsequent decrease in catalytic activity.

3.3.3 Electrochemical active area and impedance analysis

Double-layer capacitance (C_{dl}) is widely used to estimate the electrochemically active area of catalysts, as shown in Figure 5. A larger C_{dl} value indicates a larger active area and a greater number of active sites [19]. The test results show that the C_{dl} value of 15% Eu-Ni-Fe LDH is $12.94 \text{ mF}\cdot\text{cm}^{-2}$, which is significantly higher than that of pristine Ni-Fe LDH ($9.26 \text{ mF}\cdot\text{cm}^{-2}$). This result confirms that Eu doping can effectively increase the electrochemically active area of the material, expose more active sites, and thus enhance its catalytic activity. EIS results show that the impedance arc radius of 15% Eu-Ni-Fe LDH is significantly smaller

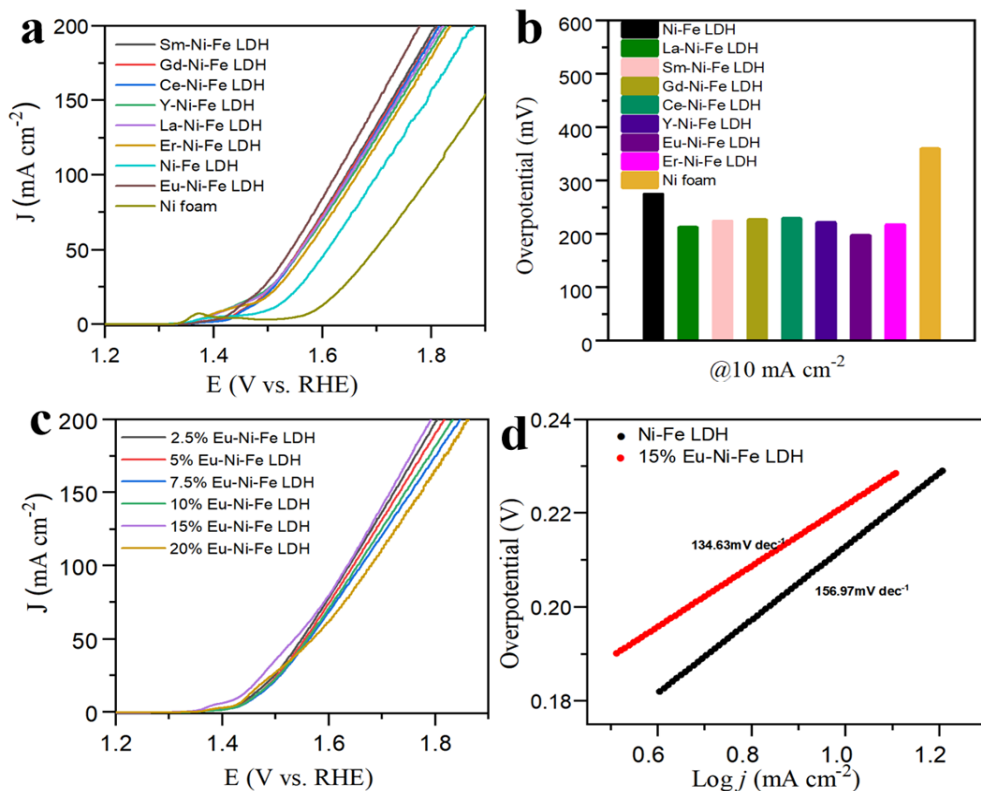


Figure 4: (a) and (b) represent the LSV curves of the original Ni-Fe LDH and the 7 types of Ni-Fe LDH doped with rare earth elements, respectively, and the overpotential at a current density of 10 mA·cm⁻²; (c) shows the LSV curves of various Eu-Ni-Fe LDHs; and (d) presents the Tafel slope curves of the original Ni-Fe LDH and the 7 types of Ni-Fe LDH doped with rare earth elements.

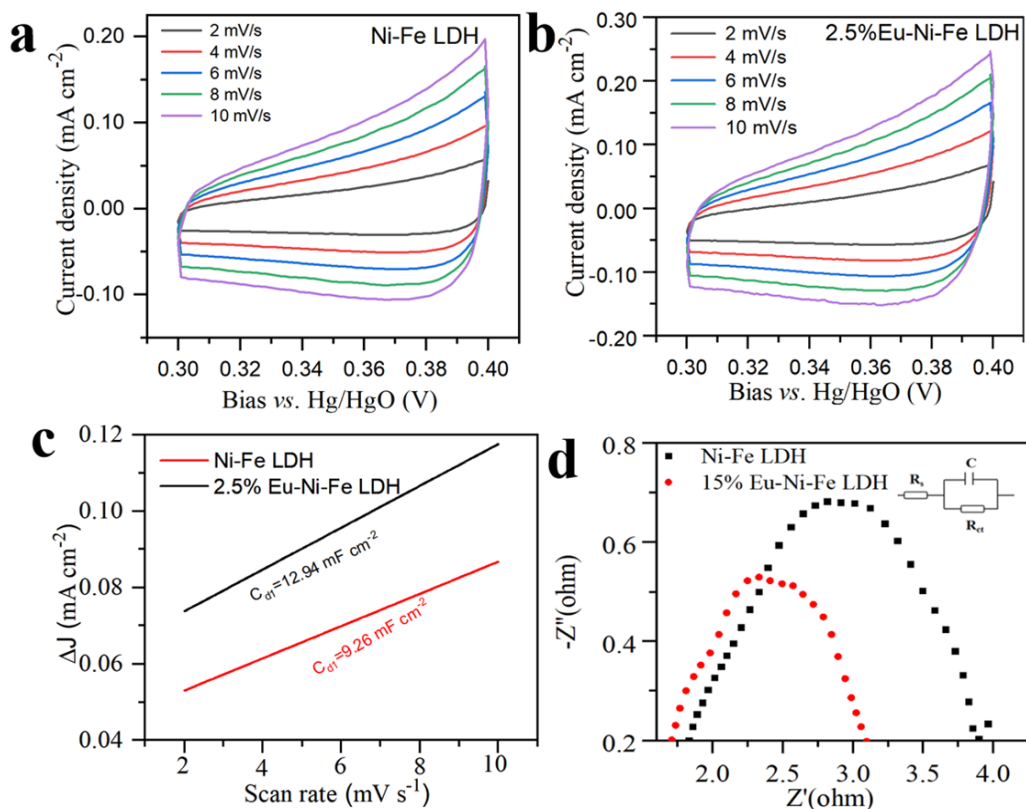


Figure 5: (a) and (b) Cyclic voltammograms of electrodes with different scanning rates (2, 4, 6, 8, 10 mv·s⁻¹); (c) C_{dl} values of the materials under different scanning rates; and (d) electrochemical impedance diagram.

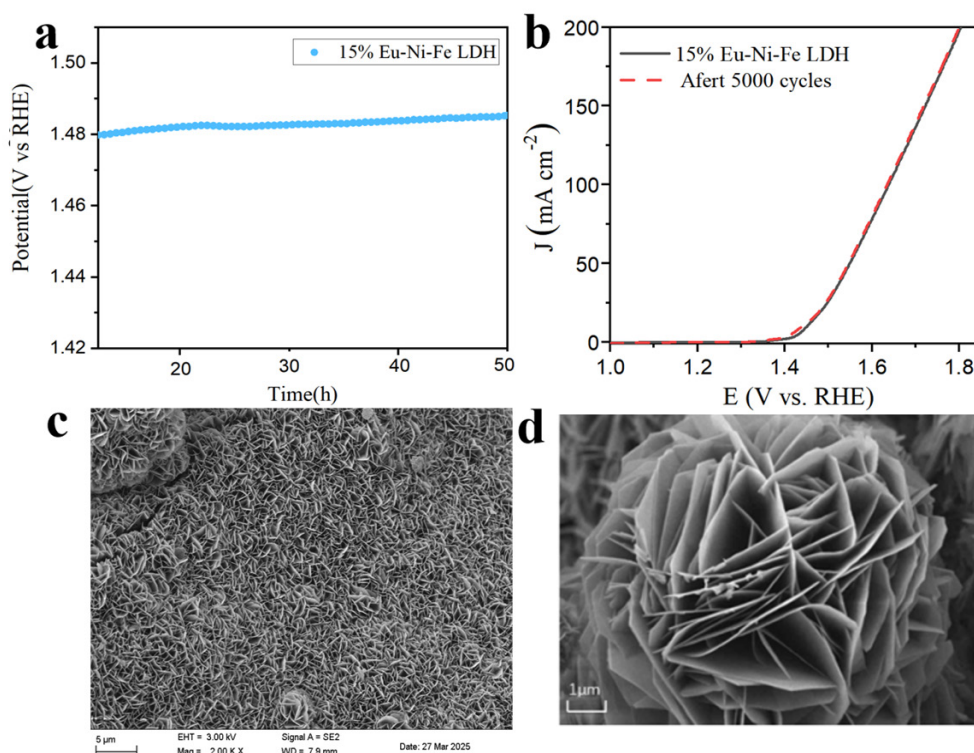


Figure 6: (a) The stability of 15% Eu-Ni-Fe LDH at a current density of $10 \text{ A}\cdot\text{cm}^{-2}$; (b) the LSV curves of 15% Eu-Ni-Fe LDH before and after 5,000 CV cycles; (c) and (d) the SEM images of 15% Ni-Fe LDH after the OER reaction.

than that of pristine Ni-Fe LDH, indicating a lower charge transfer resistance (R_{ct}) and higher electrical conductivity. This is because Eu doping can modulate the electronic structure of Ni-Fe LDH, reduce charge transfer resistance, and accelerate electron transfer rate, thereby improving the catalytic performance of the material.

3.3.4 Stability analysis

Catalyst stability is a critical indicator for its practical industrial application. Figure 6 shows the stability test results of 15% Eu-Ni-Fe LDH. During a 50-hour constant current test at a current density of $10 \text{ mA}\cdot\text{cm}^{-2}$, the current density of the sample fluctuated slightly, demonstrating excellent performance retention. After 5,000 CV cycles, the LSV polarization curve is almost identical to the initial curve without obvious shifts. SEM images further confirm that the sample maintains a complete two-dimensional nanosheet stacked structure after cycling, without collapse or agglomeration. These results show that 15% Eu-Ni-Fe LDH possesses excellent long-term stability, making it suitable for practical water electrolysis applications.

4. CONCLUSIONS

In summary, seven rare earth ion-doped Ni-Fe LDH electrocatalysts were successfully synthesized via a simple and low-cost one-pot method. Systematic investigations into the effects of rare earth element types and Eu doping content on the material structure and OER catalytic performance revealed that rare earth ions can be uniformly doped into the layered structure of Ni-Fe LDH without compromising its crystal structure or morphology, while maintaining excellent crystallinity. Among all rare earth dopants, Eu doping achieves the optimal OER catalytic activity, with the 15% Eu-doped Ni-Fe LDH demonstrating the best performance in 1.0 mol/L KOH electrolyte, specifically an overpotential of 196.8 mV at $10 \text{ mA}\cdot\text{cm}^{-2}$, a Tafel slope of $134.63 \text{ mV}\cdot\text{dec}^{-1}$, and a C_{dl} of $12.94 \text{ mF}\cdot\text{cm}^{-2}$. Moreover, Eu doping significantly enhances the catalytic activity and stability of Ni-Fe LDH by regulating its electronic structure, increasing the electrochemically active area, reducing charge transfer resistance, and accelerating OER

reaction kinetics, enabling the 15% Eu-doped sample to maintain stable performance after a 50-hour constant current test and 5,000 CV cycles. This work offers a novel strategy for the design of high-performance LDH-based OER catalysts and broadens the application prospects of rare earth elements in the field of electrocatalysis.

REFERENCES

- [1] Dawood, F., Anda, M., Shafiullah, G.M., et al. 2020. Hydrogen production for energy: An overview. *International Journal of Hydrogen Energy*, 2020, 45(7): 3847-3869.
- [2] Shulga, R.N., Petrov, A.Y., Putilova, I.V., et al. 2020. The Arctic: Ecology and hydrogen energy. *International Journal of Hydrogen Energy*, 2020, 45(11): 7185-7198.
- [3] Guo, T., Li, L., Wang, Z., et al. 2022. Recent development and future perspectives of amorphous transition metal-based electrocatalysts for oxygen evolution reaction. *Advanced Energy Materials*, 2022, 12: 34-65.
- [4] Hughes, J.P., Clipsham, J., Chavushoglu, H., et al. 2021. Polymer electrolyte electrolysis: A review of the activity and stability of non-precious metal hydrogen evolution reaction and oxygen evolution reaction catalysts. *Renewable and Sustainable Energy Reviews*, 2021, 139: 110709.
- [5] Sun, Z., Wang, G., Koh, S.W., et al. 2020. Solar-driven alkaline water electrolysis with multifunctional catalysts. *Advanced Functional Materials*, 2020, 30: 2002138.
- [6] Li, X., Hao, X., Abudula, A., et al. 2016. Nanostructured catalysts for electrochemical water splitting: Current state and prospects. *Journal of Materials Chemistry A*, 2016, 4: 11973-12000.
- [7] Khan, M.A., Zhao, H., Zou, W., et al. 2018. Recent progresses in electrocatalysts for water electrolysis. *Electrochemical Energy Reviews*, 2018, 1(4): 483-530.

- [8] Anantharaj, S., Karthick, K., Kundu, S., et al. 2017. Evolution of layered double hydroxides (LDH) as high performance water oxidation electrocatalysts: A review with insights on structure, activity and mechanism. *Materials Today Energy*, 2017, 6: 1-26.
- [9] Chen, H., Liang, X., Liu, Y., et al. 2020. Active site engineering in porous electrocatalysts. *Advanced Materials*, 32(44): 2002435.
- [10] Jung, S.Y., Kang, S., Kim, K., et al. 2021. Sulfur-incorporated nickel-iron layered double hydroxides for effective oxygen evolution reaction in seawater. *Ceramist*, 2021, 568: 150965.
- [11] Zhou, Q., Chen, Y.P., Zhao, G.Q., et al. 2018. Active-site-enriched iron-doped nickel/cobalt hydroxide nanosheets for enhanced oxygen evolution reaction. *ACS Catalysis*, 2018, 8: 5382-5390.
- [12] Han, L.P., Yao, R.Q., Wan, W.B., et al. 2019. Hierarchical nanoporous intermetallic compounds with self-grown transition-metal hydroxides as bifunctional catalysts for the alkaline hydrogen evolution reaction. *Journal of Materials Chemistry A*, 2019, 7(45): 25925-25931.
- [13] Xu, H., Shan, C., Wu, X., et al. 2020. Fabrication of layered double hydroxide microcapsules mediated by cerium doping in metal-organic frameworks for boosting water splitting. *Energy & Environmental Science*, 2020, 13: 2949-2956.
- [14] Wang, M., Jiang, J., Ai, L., et al. 2018. Layered bimetallic iron-nickel alkoxide microspheres as high-performance electrocatalysts for oxygen evolution reaction in alkaline media. *ACS Sustainable Chemistry & Engineering*, 2018: 6117-6125.
- [15] Xiong, Z., Wang, W., Li, J., et al. 2022. The synergistic promotional effect of W doping and sulfate modification on the NH₃-SCR activity of CeO₂ catalyst. *Molecular Catalysis*, 2022, 522: 112250.
- [16] Zheng, Y., Deng, H., Feng, R.Z.L., et al. 2020. Triethanolamine-assisted synthesis of NiFe layered double hydroxide ultrathin nanosheets for efficient oxygen evolution reaction. *Scientific Reports*, 2020, 10: 1-12.
- [17] He, Y., Zhou, W., Xu, J., et al. 2022. Rare earth-based nanomaterials for supercapacitors: Preparation, structure engineering and application. *ChemSusChem*, 2022, 15: e202200469.
- [18] Li, L., Wang, P., Shao, Q., et al. 2020. Metallic nanostructures with low dimensionality for electrochemical water splitting. *Chemical Society Reviews*, 2020, 49: 3072-3106.
- [19] Lei, C., Li, W., Wang, G., et al. 2021. Improving the catalytic efficiency of NiFe-LDH/ATO by air plasma treatment for oxygen evolution reaction. *Chemical Research in Chinese Universities*, 2021, 37(3): 293-297.
- [20] Du, S., Ren, Z., Wang, X., et al. 2022. Controlled atmosphere corrosion engineering toward inhomogeneous NiFe-LDH for energetic oxygen evolution. *ACS Nano*, 2022, 16: 7794-7803.

